Anadolu Üniversitesi Bilim ve Teknoloji Dergisi A- Uygulamalı Bilimler ve Mühendislik
Anadolu University Journal of Science and Technology A- Applied Sciences and Engineering

2017 - Volume: 18 Number: 3
Page: 611- 623
DOI: 10.18038/aubtda.292569
Received: 16 February 2017 Revised: 01 June 2017 Accepted: 03 July 2017

A FLUORESCENT FILM PROBE BASED ON SCHIFF BASE FOR DETERMINATION OF Fe^{3+} IONS

Musa KAMACI *

Department of Chemistry, Faculty of Sciences and Letters, Piri Reis University, 34940 Tuzla, Istanbul, Turkey

ABSTRACT

In this paper, fluorescent film probe based on Schiff base was easily prepared and it was used as fluorescence chemosensor for the detection of transition metal ions in aqueous medium. Fluorescence measurements were done using fluorescence spectroscopy and the obtained results showed that the proposed sensor have two emission maxima at 539 and 582 nm. In addition, the proposed film sensor exhibited high sensitivity and selectivity to Fe^{3+} cation in the mentioned wavelengths. Quantum yield of the fluorescent sensor was also calculated as 3.24%. The limit of detection (LOD) of the chemosensor was calculated using fluorescence titration method and it determined as 53.7 and 3.53 µM at 539 and 582 nm. Fluorescence data indicated that the proposed sensor has potential application to determination of Fe^{3+} cations in deionized water without interference of the used other metal cations.

Keywords: Schiff base, Chemosensor, Fe (III) ion, Fluorescent sensor, pH effect

1. INTRODUCTION

In recent years, many traditional techniques such as inductively coupled plasma-atomic emission spectroscopy (ICP-AES) [1, 2], atomic absorption spectroscopy (AAS) [3], electrochemical methods [4], high performance liquid chromatography (HPLC) [5] and fluorescence spectroscopy [6, 7] were improved. These techniques were also used to determination of transition metal ions such as Fe^{3+}, Cu^{2+}, Hg^{2+}, Co^{2+} in water, biological, medical, industrial and environmental medium. Among these techniques, fluorescence spectroscopy has far superior properties than the other techniques such as rapid response, low cost, real-time monitoring, easy operation and high sensitivity [8-10].

Detection of Fe^{3+} ion in various medium has attracted great interest due to biological importance of this metal ion [11]. This transition metal ion plays an important role in numerous biological processes such as DNA or RNA synthesis [12, 13], electron transfer [14], enzymatic reactions [15] and oxygen carrier in hemoglobin [16]. In addition, both deficiency and overload of Fe^{3+} ion cause different disorders. Deficiency of this ion leads to anemia, diabetes, heart disease, Parkinson's disease, cancer, and dysfunction of some organs such as liver, heart and pancreas [17, 18]. Moreover, accumulation of Fe^{3+} causes Alzheimer's disease, oxidative stress and neurodegenerative diseases [19, 20]. Therefore, the development of the fluorescence sensor for the detection of Fe^{3+} ion in different medium is quite important.

Herein, fluorescent sensor based on Schiff base was easily fabricated via dip-coating technique and it was used for the detection of transition metal ions. Fluorescent film probe exhibited high fluorescence sensitivity and selectivity toward Fe^{3+} ion among a series of metal cations such as Al^{3+}, Ba^{2+}, Cd^{2+}, Co^{2+}, Cu^{2+}, Hg^{2+}, Mn^{2+}, Mg^{2+}, Ni^{2+}, Pb^{2+}, Sn^{2+} and Zn^{2+} in aqueous medium.

*Corresponding Author: mkamaci@pirireis.edu.tr

2. EXPERIMENTAL

2.1. Reagents, Solvents and Instruments

All reagents and solvents in this work were obtained commercially and they were used as received without further purification. *p*-Phylenediamine, 5-nitro vanillin, acetic acid (CH_3COOH), acetonitrile (MeCN), boric acid, chloroform ($CHCl_3$), dimethylformamide (DMF), ethanol (EtOH), hydrochloric acid (HCl), phosphoric acid (H_3PO_4), sodium hydroxide (NaOH), tetrahydrofurane (THF) were purchased from Sigma-Aldrich. $AlCl_3$, $Ba(NO_3)_2$, $Cd(CH_3COO)_2x2H_2O$, $Co(CH_3COO)_2x4H_2O$, $Cu(CH_3COO)_2xH_2O$, $FeNO_3$, $HgCl_2$, $Mn(CH_3COO)_2xH_2O$, $Mg(SO_4)x7H_2O$, $Ni(CH_3COO)_2x4H_2O$, $Pb(CH_3COO)_2x3H_2O$, $SnCl_2x6H_2O$ and $Zn(CH_3COO)_2x2H_2O$ were supplied from Merck Chemical Co. (Germany).

^1H and ^{13}C-NMR spectra (Bruker AC FT-NMR spectrometer operating at 400 and 100.6 MHz, respectively) were recorded by using deuterated DMSO-d_6 as a solvent at 25°C. All fluorescence measurements were carried out using Perkin-Elmer LS 55 fluorescence spectrometer. Fluorescence spectra were measured using excitation at 400 nm with a high energy pulsed Xenon source and a 5 nm width. UV-vis absorption spectra of PAMPN fluorescent film probe were recorded using Perkin-Elmer Lambda 25 UV-vis spectrophotometer in the presence of different molarity Fe^{3+} ion at room temperature.

2.2. Synthesis of Schiff Base (PAMPN)

Figure 1 shows the schematic synthesis route of Schiff base [4,4'-((1E,1'E)-(1,4-phenylenebis(azanylylidene))bis(methanylylidene))bis(2-methoxy-6-nitrophenol)]. Schiff base was abbreviated as PAMPN and it was synthesized via condensation reaction of *p*-phylenediamine with 5-nitro vanillin as in the literature [21]. **Yield:** 91%; **^{1}H-NMR** (400 MHz, DMSO-d_6): 8.60 (hydroxyl, -O<u>H</u>), 8.14 (imine, –N=C<u>H</u>), between 7.58 and 6.67 (Ar-C<u>H</u>) and 3.81 (methoxy, -OC<u>H</u>$_3$); **^{13}C-NMR** (100.6 MHz, DMSO-d_6): 164.25 (hydroxyl, -<u>C</u>-OH), 153.04 (imine, –N=<u>C</u>H), 133.38 (nitro, -<u>C</u>-NO_2), in the range 114.23 to 148.14 (Ar-<u>C</u>H) and 55.97 (methoxy, -O<u>C</u>H$_3$)

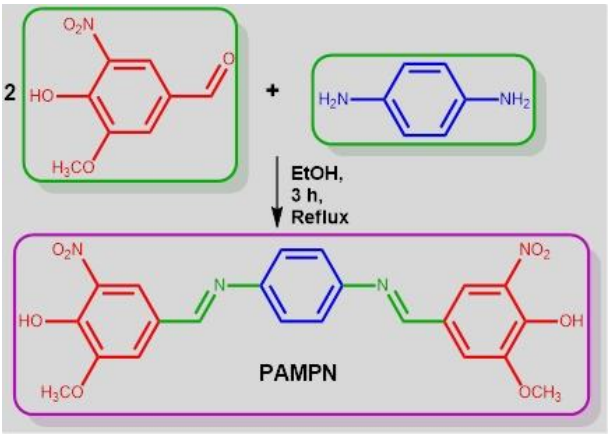

Figure 1. Synthesis route of PAMPN

2.3. Preparation of Standard Stock Solution

Stock solution (1.0 mM) of a series of metal cations such as Al^{3+}, Ba^{2+}, Cd^{2+}, Co^{2+}, Cu^{2+}, Fe^{3+}, Hg^{2+}, Mn^{2+}, Mg^{2+}, Ni^{2+}, Pb^{2+}, Sn^{2+} and Zn^{2+} was prepared using de-ionized water their nitrate, chloride or acetate salts. These prepared stock solutions were also used in all measurements.

2.4. Preparation of Buffer Solution

Brittion-Robinson buffer solution was used pH measurements. In these measurements, this buffer solution was prepared by mixing 40 mM acetic acid, 40 mM boric acid and 40 mM phosphoric acid. Also, this buffer solution was used to adjust to desired pH with 20 mM NaOH or 0.20 mM HCl. The desired pH value of the fluorescent sensor is in the range from 7 to 9.

2.5. Fabrication of Fluorescent Film Probe

Schiff base film was prepared by dip-coating technique and film coated on transparent polyester surface. In order to obtain high-quality thin PAMPN film, the transparent polyester surface was carefully cleaned with methanol, acetonitrile and deionized water and, dried in desiccator before use. Then, this cleaned surface was used as substrate to coat film. The typical coating process of PAMPN film was described as follows: a polyepoxide layer was coated on polyester surface from its chloroform solution by dip-coating technique with a withdraw rate 100 mm/min and polyepoxide layer coated plate was dried at room temperature overnight in desiccator. This coated was carried out due to compensate for weak adherence of Schiff base onto polyester plate. Finally, Schiff base was coated on polyepoxide coated plate by dip-coating technique with a withdraw rate 100 mm/min and the coated film was dried at room temperature overnight in desiccator. Concentration of Schiff base solution was adjusted as 50 mM in this coating process.

3. RESULTS AND DISCUSSION

3.1. Photoluminescence (PL) properties of PAMPN

Excitation and emission spectra of PAMPN were measured using fluorescence spectroscopy in deionized water at room temperature (Figure 2). PAMPN exhibits two excitation bands at 327 and 398 nm. Similarly, Schiff base exhibits two emission bands at 539 and 586 nm when excited at 400 nm. Moreover, emission intensity of PAMPN was measured at 229 and 305 a.u. for 539 and 586 nm, respectively.

Stoke shift (Δ_{ST}) is described as the difference between the maximum wavelengths between the excitation and emission spectra [22]. Stokes shift (Δ_{ST}) value of PAMPN film probe was calculated between 212 and 184 in the mentioned emission wavelengths. These results showed that the proposed sensor has quite large Stokes shift value due dual excitation and emission maxima. As known, Stokes shift is a very important parameter for fluorescence probe or sensor due to it attributed to the interaction of the environment with chromosphere groups [23, 24].

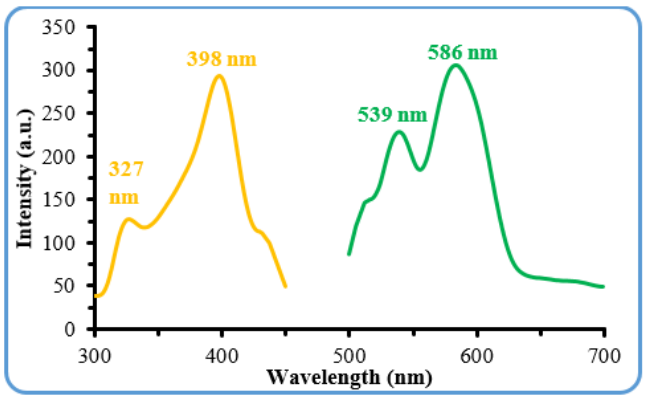

Figure 2. Excitation and emission spectra of PAMPN in deionized water

Quantum yield of PAMPN sensor was calculated as in the literature using the following equation [25]:

$$\Phi_f = \Phi_f^0 \frac{F_s.A_o.n_s^2}{F_o A_s n_o^2} \quad (1)$$

where F_o, A_o and n_o are integrated fluorescence intensity, absorbance and refractive index of reference, respectively. F_s, A_s and n_s are integrated fluorescence intensity, absorbance and refractive index of polymer solutions, respectively. To calculate quantum yield of PAMPN fluorescence sensor, Fluorescein solution in ethanol was used as reference ($\Phi_f^0 = 92\%$) and quantum yield of Schiff base probe calculated as 3.24%.

3.2. Metal ions Sensing Properties

Metal cation sensing ability of the proposed film probe was studied in the presence of a series of metal cations such as Fe^{3+}, Pb^{2+}, Mn^{2+}, Ni^{2+}, Sn^{2+}, Co^{2+}, Cu^{2+}, Cd^{2+}, Mg^{2+}, Al^{3+}, Pb^{2+}, Pb^{2+} and Pb^{2+} (Figure 3).

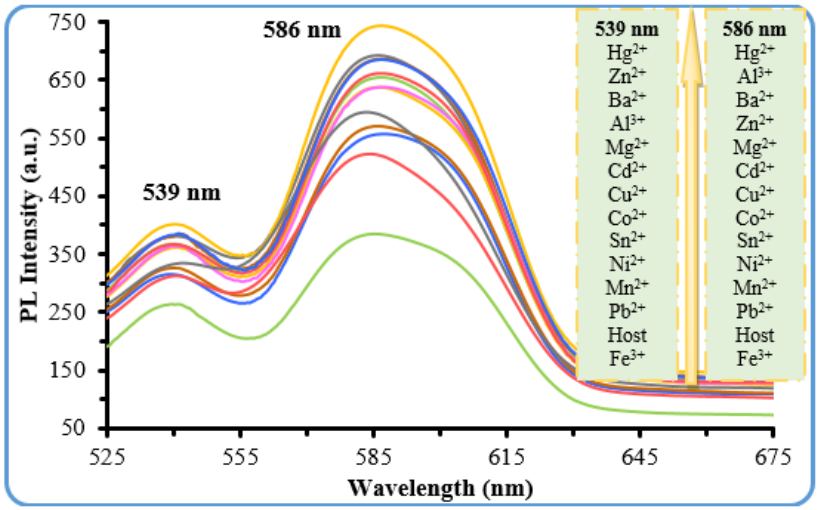

Figure 3. Emission spectra of PAMPN probe in the presence of different metal ions

The obtained data were also summarized in Table 1. Concentration of metal cations was adjusted as 1.0 mM in the mentioned measurements. When 3 mL metal cation solutions (1 mM) were added to fluorescence probe, emission intensity of PAMPN was decreased in the presence of iron (III) cation whereas emission intensity of PAMPN was increased in the presence of the other metal cations both 539 and 586 nm. These obtained results showed that PAMPN fluorescent probe was used to detection of Fe^{3+} cation in aqueous solution at these wavelengths.

Table 1. Emission spectral data of PAMPN in presence of different metal ions

Wavelength (nm)		Emission Intensity of Metal Ions												
	Host	Al^{3+}	Ba^{2+}	Cd^{2+}	Co^{2+}	Cu^{2+}	Fe^{3+}	Hg^{2+}	Mg^{2+}	Mn^{2+}	Ni^{2+}	Pb^{2+}	Sn^{2+}	Zn^{2+}
539	382	381	381	367	362	364	265	402	367	316	326	312	332	383
586	482	692	687	654	638	638	385	744	662	558	571	521	591	686

3.3. Fe^{3+} Cation Concentration Effect on PAMPN

In order to detection of iron (III) cation concentrations effect on PAMPN film probe, PL spectra of film probe were measured in the presence of different Fe^{3+} cation concentrations in the range 62.5 to 1000

µM (Figure 4). These PL spectra showed that as Fe^{3+} ion concentration increased emission intensity of PAMPN fluorescent probe continuously decreased both 539 and 586 nm.

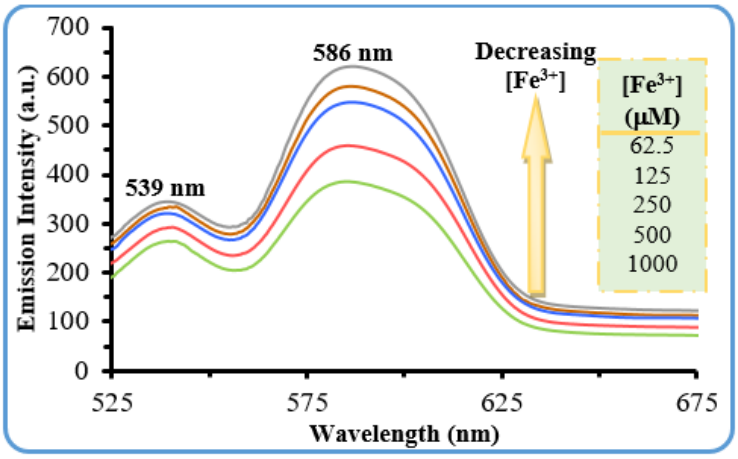

Figure 4. Emission spectra of PAMPN in the presence of different Fe^{3+} ion concentration

3.4. UV-vis Spectra of PAMPN Fluorescent Probe

UV-Vis absorption spectra of PAMPN films were measured in the presence of different Fe^{3+} cation concentrations (Figure 5). As can be seen in Figure 4, absorbance of PAMPN probe was increased as Fe^{3+} cation concentration decreased in the range 1.0 to 0.00156 µM.

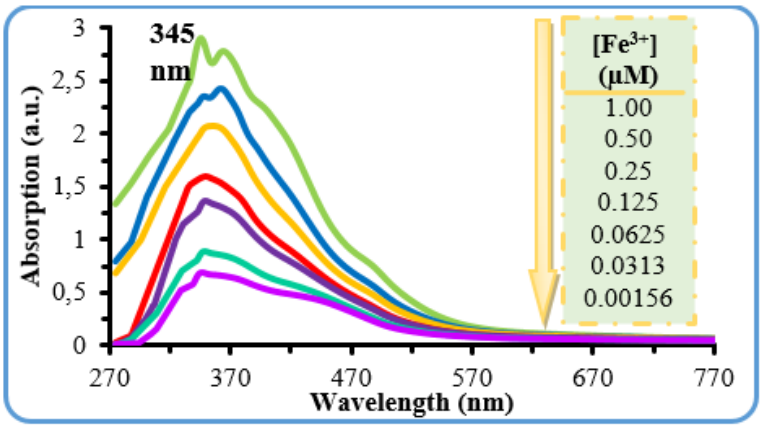

Figure 5. UV-Vis spectra of PAMPN in the presence of different molarity Fe^{3+}

3.5. Determination of Limit of Detection (LOD)

To determine LOD value of PAMPN film probe, the difference (ΔF) between the emission intensity of tested metal cation (F) and emission intensity of metal-free PAMPN film (F_o) *versus* wavelength of spectra were obtained using fluorescence measurements (Figure 6). The obtained equations to calculate LOD value were given in Eqs. 2 and 3.

$$\Delta F = -82925[Fe^{3+}] + 343.33 \quad \text{(at 541 nm, R= 0.966)} \quad (2)$$

$$\Delta F = -243376[Fe^{3+}] + 612.71 \quad \text{(at 578 nm, R= 0.951)} \quad (3)$$

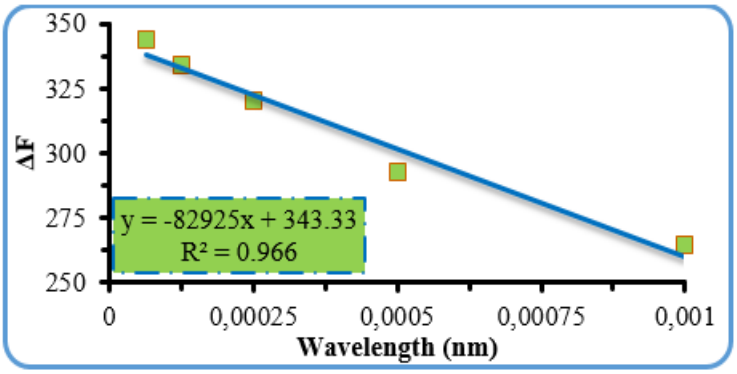

(a)

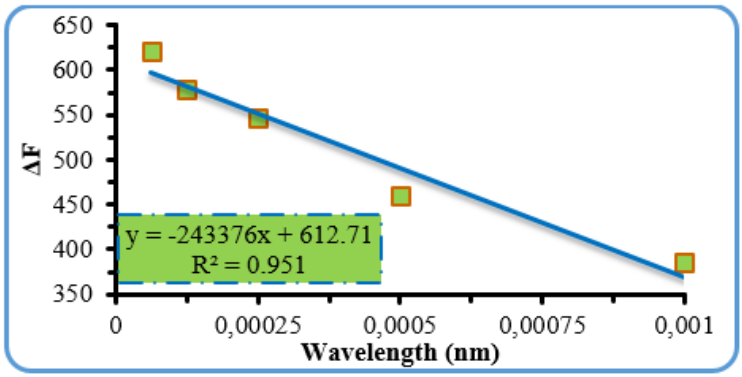

(b)

Figure 6. Calibration curves for determination of Fe^{3+} ions by the proposed fluorescent probe (a) at 539 and (b) at 586 nm.

These results showed that a good linearity response was obtained with the regression coefficients R_1= 0.966 and R_2= 0.951 for 539 and 586 nm, respectively. According to these results, the proposed fluorescent sensor has potential prospects as a selective detector for Fe^{3+} cation in aqueous medium.

Moreover, limit of detection (LOD) value of PAMPN chemosensor was calculated using fluorescence titration method as in the literature. Firstly, standard deviation (σ_{bi}) of PAMPN probe without metal cations was measured 10 times in deionized water and σ_{bi} determined as 1.484 and 0.286 for 539 and 582 nm, respectively.

LOD value of PAMPN chemosensor was calculated as the following Eq. 4 [26]:

$$\text{LOD} = \frac{3\sigma bi}{m} \tag{4}$$

where m is the slope the obtained from Figure 6 and LOD values of PAMPN film probe was calculated as 53.7 and 3.53 µM for the mentioned wavelengths.

3.6. Determination of the Effective Quenching Constant (K_a)

The effective quenching constant (K_a) of Schiff base film sensor with Fe^{3+} cation was determined as following equation [27]:

$$\frac{F_o}{\Delta F} = \frac{1}{f_a} + \frac{1}{f_a K_a [PAMPN]} \tag{5}$$

where K_a and f_a are the effective quenching constant and the fraction of accessible fluorophore, respectively, and ΔF is the fluorescence intensity difference between absence and presence of Fe^{3+} cation at 539 and 582 nm (Figure 7). $1/f_a.K_a$ value of fluorescence sensor was calculated to the slope of graph. The effective quenching constant (K_a) of Schiff base probe was calculated as $1.81x10^{-3}$ and $2.35x10^{-3}$ M^{-1} at 539 and 582 nm, respectively.

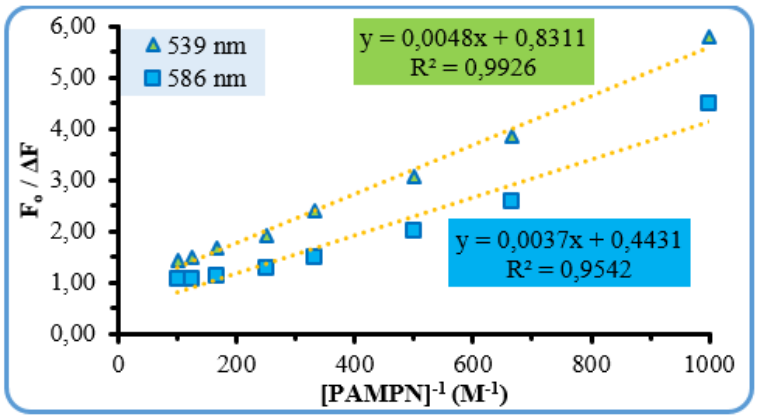

Figure 7. Constant plot of PAMPN

3.6. Interference Study

Interference studies of the proposed sensor film were done due to determine interference or anti-interference ability of the tested metal cations on Schiff base (Figure 8). Concentration of the tested metal cations was adjusted as 1.0 mM in these measurements. According to Figure 7, iron (III) cation has the lowest relative emission intensity when compared to the other metal cations. Moreover, the other metal cations were not induced significant fluorescence change at 539 and 586 nm.

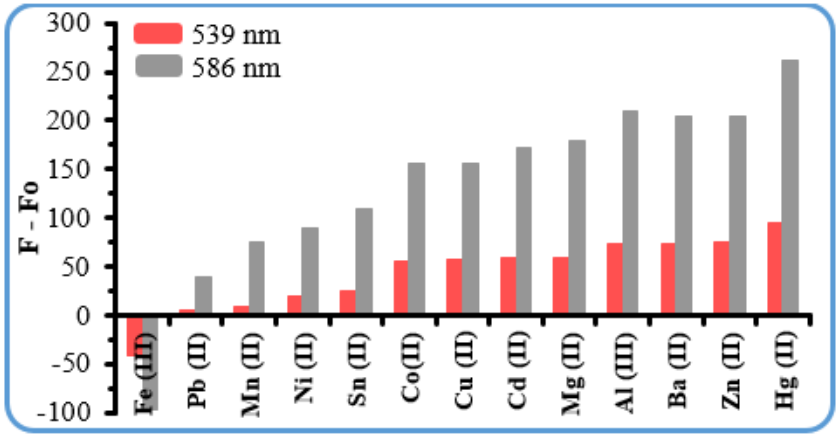

Figure 8. Change in the relative intensity of probe upon addition of various metal ions in deionized water at 539 and 586 nm for PAMPN.

3.7. Quenching ion effect on PAMPN Probe

Figure 9 shows quenching ion effect on the fluorescent film. To determine the quenching ion effect on PAMPN film, 1 mg metal salt and PAMPN-Fe^{3+} ion complex were used. Also, Fe^{3+} ion concentration was adjusted as 1 mM in these measurements. As can be seen in Figure 9, the used metal cations were

not significantly quenched on Schiff base sensor and these metal cations brought about only a bit changes in the emission intensities.

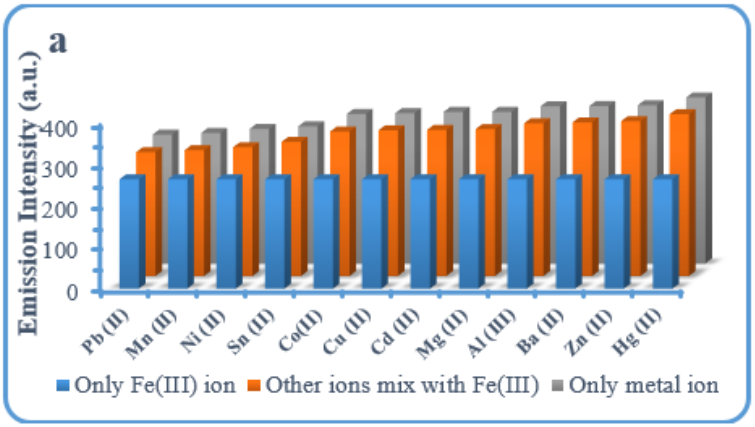

(a)

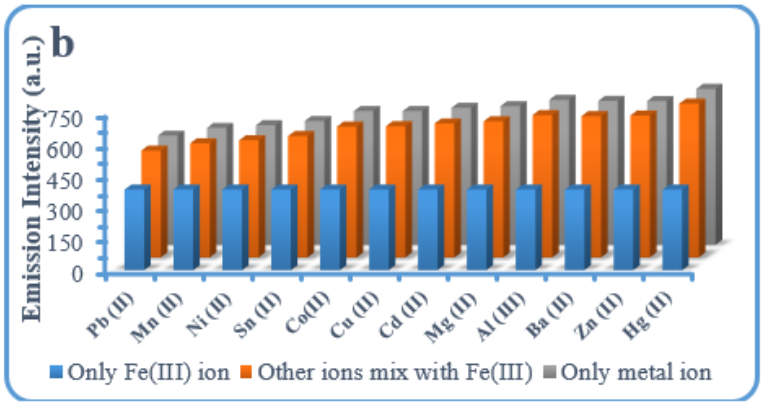

(b)

Figure 9. Quenching ion effect on PAMPN probe (a) at 539 and (b) at 586 nm

3.8. pH Effect on PAMPN Fluorescent Film

pH is one another important parameter for the sensor. Due to the determine pH effect on PAMPN fluorescent film sensor, emission spectra of PAMPN-Fe^{3+} cation complex were measured at different pH. pH effect on the fluorescent sensor was studied using Britton-Robinson (B-R) buffer solution between 2 to 12 in these measurements and pH solutions were set to the desired value using HCl or NaOH solutions. Also, Fe^{3+} cation concentration was adjusted as 1.0 mM (Figure 10). According to Figure 10, emission intensities of PAMPN-Fe^{3+} cation complex were not significantly changed at different pH values and the proposed sensor was stable toward to pH changes. In addition, Schiff base fluorescent sensor was truly pH-independent in the range 6 to 9 and 5 to 9 at 539 and 586 nm, respectively. These results indicated that the fluorescent chemsensor can work over a broad pH range.

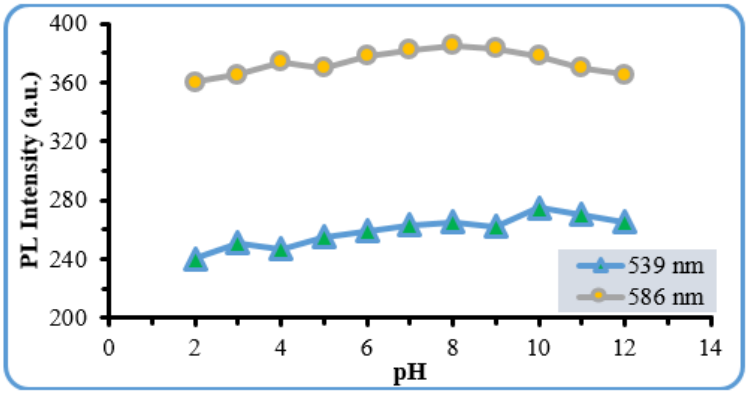

Figure 10. pH effect on PAMPN fluorescent film probe in the presence of Fe^{3+} ion

3.9. Reusability of Fluorescence Films

Figure 11 shows reusability property of PAMPN sensor. Reusability measurements of PAMPN fluorescent sensor were done in B-R buffer solution at pH= 7.0. Also, to determine the reusability of fluorescent film, PAMPN film was washed 10 mL deionized water three times before every measurements. The reusability results showed that emission intensity of PAMPN was decreased 1.32% and 2% for 539 and 586 nm after ten washing-testing cycles, respectively.

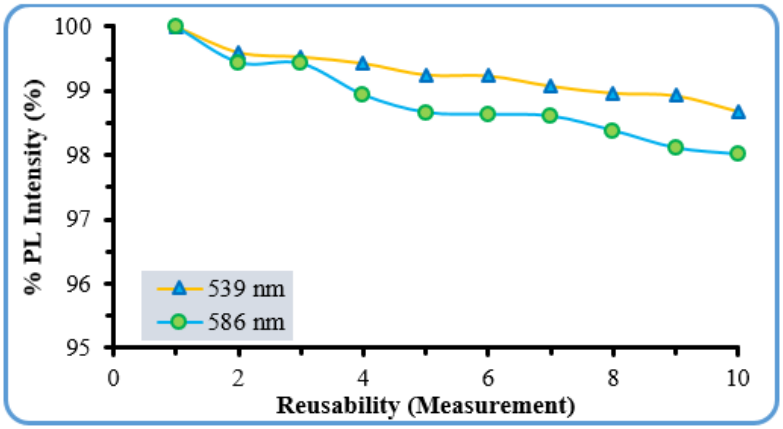

Figure 10. Reusability of PAMPN probe.

3.10. Binding Model and Responsive Mechanism

Huckel calculation method was used to indicate binding model between PAMPN film probe and iron (III) cation [28]. According to the structure of PAMPN, it contains imine nitrogen (-N=CH), hydroxyl (-OH), methoxy ($-OCH_3$) oxygens and nitro nitrogen ($-NO_2$) as chromophore group. Huckel charges of -N=CH, -OH and $-OCH_3$ were calculated as - 0.090, -0.280 and - 0.187, respectively, while $-NO_2$ was calculated as + 1.220. Figures 12a and b show 3D image of PAMPN and Huckel charge density of choromophore groups. As can be seen in Figure 12b, imine (-N=CH) group has higher charge density than the other choromophore groups. These results indicated that the possible binding model between PAMPN and Fe^{3+} cation could be mainly carried out imine nitrogen, hydroxyl and methoxy oxygens.

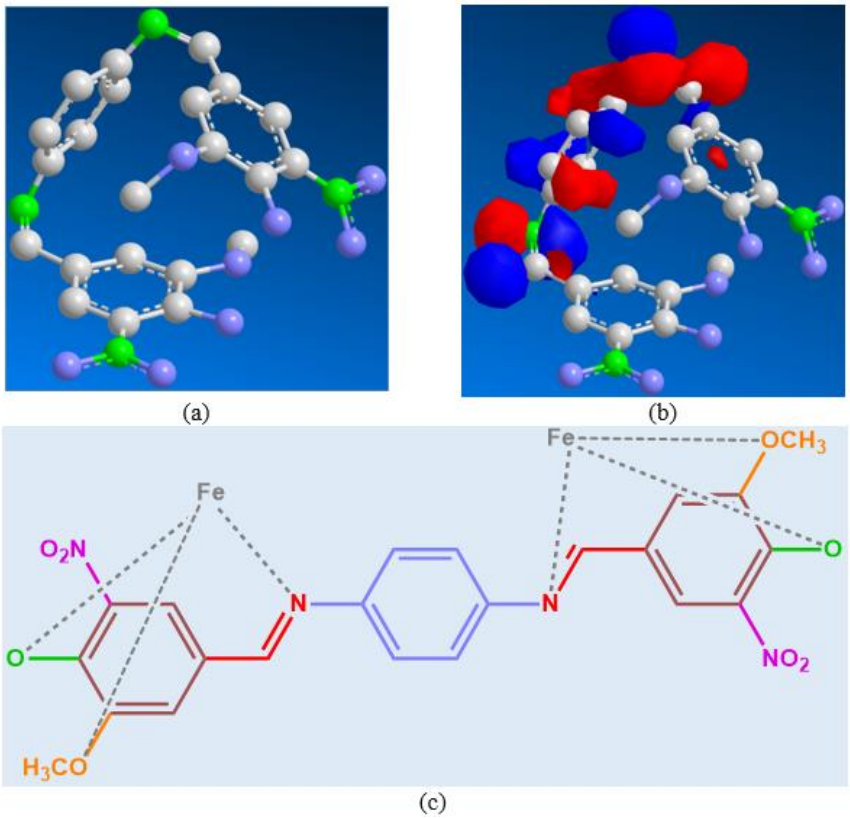

Figure 12. (a) 3D image of PAMPN, (b) Huckel charge of PAMPN, (c) binding mechanism between PAMPN and Fe (III) [Grey: carbon, green: oxygen, purple: nitrogen atoms, hydrogen atoms are not shown].

3.11. Photostability of Film Probes

To investigate photostability of PAMPN fluorescent probe, emission intensity of probe was measured both 539 and 582 nm under a xenon light source in deionized water during 30 minutes (Figure 13).

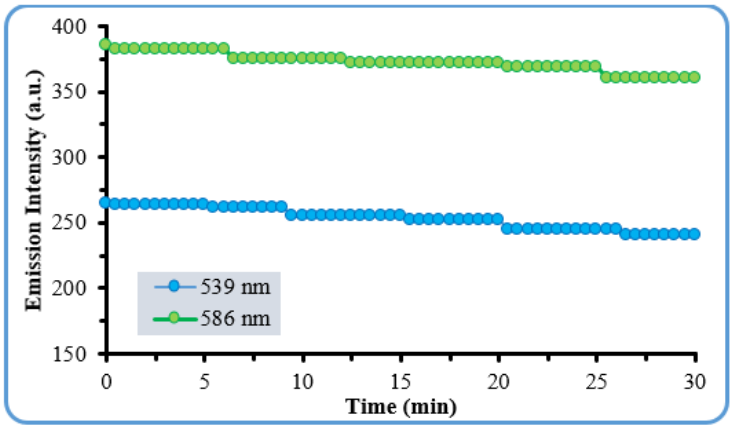

Figure 13. Photostability curves of PAMPN at 539 ad 586 nm

Moreover, photostability data were summarized in Table 2. According to Table 2 and Figure 12, emission intensity of PAMPN fluorescent film was decreased 0.75, 3.77, 4.91 and 9.43% for 539 nm, 0.78, 2.60, 3.38 and 6.49% for 586 nm after 5, 10, 20 and 30 minutes, respectively. The obtained photostability results clearly indicated that PAMPN fluorescent probe has been showed quite photostable property.

Table 2. Photostability data of PAMPN in deionized water in presence of Fe^{3+} ion

Wavelengths (nm)	Time (min)	0	5	10	15	20	25	30
539	Intensity	265	263	255	255	252	245	240
	Degradation (%)	-	0.75	3.77	3.77	4.91	7.55	9.43
586	Intensity	385	382	375	372	372	368	360
	Degradation (%)	-	0.78	2.60	3.38	3.38	4.42	6.49

Consequently, the proposed fluorescent sensor for the detection of Fe^{3+} ion in aqueous medium has good Stokes shift and LOD value. According to the interference and quenching effects of the tested metal ions on the sensor, the tested ions were caused only a bit change in the emission intensity of Schiff base-Fe^{3+} complex. In addition, the sensor can work over a broad pH range. These results prove that the proposed fluorescent system was successfully studied for the detection of Fe^{3+} ion in aqueous medium.

4. CONCLUSION

In this paper, fluorescent sensor based on Schiff base was easily designed using dip-coating technique. Fluorescence properties of the proposed sensor were studied using PL spectrophotometers. Schiff base exhibits two emission bands at 539 and 582 nm. Metal ion sensing property of the fluorescent film probe was studied in the presence of a series of metal cations at these emission bands. PL data showed that the proposed sensor was exhibited good sensitivity and selectivity toward Fe^{3+} cation. Stokes shift and LOD values of fluorescent sensor were calculated in the range 212 to 184 nm and 53.7 to 3.53 μM at the mentioned wavelengths, respectively. Interference ability and quenching ion effect on the proposed sensor were also investigated. The results indicated that the used metal cations lead to only a bit change in the emission intensity of PAMPN-Fe^{3+} complex. As a result, fluorescence data indicated that the proposed sensor has potential application to determination of Fe^{3+} cation in deionized water without interference of the used other metal ions.

REFERENCES

[1] Hua CJ, Zheng H, Zhang K, Xin M, Gao JR, Li YJ. A novel turn off fluorescent sensor for Fe(III) and pH environment based on coumarin derivatives: the fluorescence characteristics and theoretical study. Tetrahedron 2016; 72: 8365-8372.

[2] Antheraidis AN, Zachariadis GA, Stratis JA. Gallium trace on-line pre-concentration/separation and determination using a polyurethane foam mini-column and flame atomic absorption spectrometry. Application in aluminum alloys, natural waters and urine. Talanta 2003; 60: 929–936.

[3] Wang Y, Liu Z, Sun J, Liu X, Pei M, Zhang G. A turn-on fluorescence probe for Fe3+ based-on benzimidazo[2,1-a] benz[de]isoquinoline-7-one derivatives. J Photoch Photobio A 2017; 332: 515–520.

[4] Long Q, Wen Y, Li H, Zhang Y, Yao S. A novel fluorescent biosensor for detection of silver ions based on upconversion nanoparticles, J Fluoresc 2017; 27: 205–211.

[5] Cheng X, Yu Y, Jia Y, Duan L. Fluorescent PU films for detection and removal of Hg^{2+}, Cr^{3+} and Fe^{3+} ions. Mater Design 2016; 95: 133–140.

[6] Wei J, Ren J, Liu J, Meng X, Ren X, Chen Z, Tang F. An eco-friendly, simple, and sensitive fluorescence biosensor for the detection of choline and acetylcholine based on C-dots and the Fenton reaction. Biosens Bioelectron 2014; 52: 304–309.

[7] Dwivedi AK, Saikia G, Iyer PK. Aqueous polyfluorene probe for the detection and estimation of Fe^{3+} andinorganic phosphate in blood serum. J Mater Chem 2011; 21: 2502–2507.

[8] Wu X, Xu B, Tong H, Wang L. Phosphonate-functionalized polyfluorene film sensors for sensitive detection of iron (III) in both organic and aqueous media. Macromolecules 2010; 43: 8917–8923.

[9] Yang Y, Huo FJ, Yin C, Chao J, Zhang Y. An 'OFF-ON' fluorescent probe for specially recognize on Cys and its application in bio-imaging. Dyes Pigments 2015; 114: 105-109.

[10] Saleem M, Lee KH. Selective fluorescence detection of Cu^{2+} in aqueous solution and living cells. J Lumin 2014; 145: 843–848.

[11] Xiao W, Chen Z. Fluorescent Iron (III) Determination Based on Salicylaldehyde Functionalized Bimodal Mesoporous Silica, J Nanosci Nanotechnol 2016; 16: 12666–12670.

[12] Bhamore JR, Jha S, Singhal RK, Kailasa SK. Synthesis of water dispersible fluorescent carbon nanocrystals from syzygium cumini fruits for the detection of Fe^{3+} ion in water and biological samples and imaging of fusarium avenaceum cells. J Fluoresc 2017; 27: 125–134.

[13] Wang M, Meng G, Huang Q, Qiaoling Xu Q, Guodong Liu G. A GBI@PPyNWs-based prototype of reusable fluorescence sensor for the detection of Fe^{3+} in aqueous solution. Anal Methods 2012; 4: 2653-2656.

[14] Braun V, Hantke K. Recent insights into iron import by bacteria. Curr Opin Chem Biol 2011; 15: 328–334.

[15] Cao H, Chen Z, Zheng H, Huang Y. Copper nanoclusters as a highly sensitive and selective fluorescence sensor for ferric ions in serum and living cells by imaging. Biosens Bioelectron 2014; 3: 189–195.

[16] Senol AM, Onganer Y, Meral K. An unusual "off-on" fluorescence sensor for iron(III) detection based on fluorescein–reduced graphene oxide functionalized with polyethylene imine. Sensor Actuat B 2017; 239: 343–351.

[17] Choi YW, Park GJ, Na YJ, Jo HY, Lee SA, You GR, Kim C. A single Schiff base molecule for recognizing multiple metal ions: A fluorescence sensor for Zn(II) and Al(III) and colorimetric sensor for Fe(II) and Fe(III). Sensor Actuat B 2014; 194: 343–352.

[18] Sui B, Tang S, Liu T, Kim B, Belfield KD. Novel BODIPY-based fluorescence turn-on sensor for Fe^{3+} and its bio-imaging application in living cells. ACS Appl Mater Interfaces 2014; 6: 18408-18412.

[19] Luo A, Wang H, Wang Y, Huang Q, Zhang Q. A novel colorimetric and turn-on fluorescent chemosensor for iron(III) ion detection and its application to cellular imaging. Spectrochim Acta A 2016; 168: 37-44.

[20] Bhatt KD, Gupte HS, Makwana BA, Vyas DJ, Maity D, Jain VK. Calix receptor edifice; Scrupulous turn off fluorescent sensor for Fe(III), Co(II) and Cu(II). J Fluoresc 2012; 22: 1493-1500.

[21] Kaya İ, Kamacı M. Synthesis, optical, electrochemical, and thermal stability properties of poly(azomethine-urethane)s. Prog Org Coat 2012; 74: 204–214.

[22] Aderinto SO, Xu Y, Peng H, Wang F, Wu H, Xuyang Fan X. A highly Selective Fluorescent Sensor for Monitoring Cu^{2+} Ion: Synthesis, Characterization and Photophysical Properties. J Fluoresc 2017; 27: 79–87.

[23] Kaya İ, Kamacı M. Highly selective and stable florescent sensor for Cd(II) based on poly(azomethine-urethane). J Fluoresc 2013; 23: 115–121.

[24] Kamacı M, Kaya İ. The novel poly(azomethine-urethane): Synthesis, morphological properties and application as a fluorescent probe for detection of Zn^{2+} ions. J Inorg Organomet Polym 2015; 25: 1250–1259.

[25] Shen B, Qian Y. Click synthesis, Hg^{2+} sensor and intramolecular fluorescence resonance energy transfer in novel BODIPY dendrons. Sensor Actuat B 2017; 239: 226-234.

[26] Sarkar D, Pramanik AK, Mondal TK. Coumarin based dual switching fluorescent 'turn-on' chemosensor for selective detection of Zn^{2+} and HSO_4^-: An experimental and theoretical study. RSC Adv 2014; 4: 25341-25347.

[27] Tian ZY, Song LN, Zhao Y, Zang FL, Zhao ZH, Chen NH, Xu XJ, Wang CJ. Spectroscopic study on the interaction between naphthalimide-polyamine conjugates and bovine serum albumin (BSA). Molecules 2015; 20: 16491-16523.

[28] Kamacı M, Kaya İ. 2,4-Diamino-6-hydroxypyrimidine based poly(azomethine-urethane): synthesis and application as a fluorescent probe for detection of Cu^{2+} in aqueous solution. J Fluoresc 2015; 25: 1339–1349.